Chapter 7
Synthesis and Functionalization of Mesoporous Bioactive Glasses for Drug Delivery

F. Branda

Abstract Recently Mesoporous bioactive glasses were synthesized for which outstanding applications in the biomedical field are expected. It is nowadays recognized, in fact, that microporous and mesoporous inorganic and hybrid organic-inorganic bioactive matrices and scaffolds can be produced with controlled rates of resorption and controlled surface chemistries. The type and concentration of released inorganic and organic species and their release sequence can be tuned; this is a vital requirement in stimulating cell proliferation and enhancing subsequent cell differentiation. The ability to bond to living tissues and the high pore volume allow to exploit mesoporous bioactive materials also simply for local drug delivery allowing to overcome the limitations of systemic delivery: therapeutic concentrations at the site of infection, but for short periods of time, forcing repeated dosing for longer periods.

The chapter is organized in four sections. The first one deals with synthesis and mechanism of formation of mesoporous bioactive glasses. The second one analyses the bioactive behavior. The third one is devoted to understand the specificity of bioactive response induced by the mesoporous structure. The fourth one deals with drug delivery from mesoporous bioactive glasses. In a first subparagraph the advantages of using bioactive glasses for local derivery and the construction of tissue engineering scaffolds are analysed. In the second one the complexity of therapeutics delivery from mesoporous bioactive glasses is analysed.

Keywords Mesoporous particles • Bioactivity • Scaffolds • Tissue engineering • Drug delivery

F. Branda (✉)
Dipartimento di Ingegneria Chimica, dei Materiali e della Produzione Industriale (Department of Chemical, Materials and Production Engineering) – DICMaPI, University of Naples "Federico II", P.le Tecchio, Naples, Italy
e-mail: branda@unina.it

G. Kaur (ed.), *Clinical Applications of Biomaterials*,
DOI 10.1007/978-3-319-56059-5_7

7.1 Introduction

Bioactive glasses and bioactive fixation were discovered by Hench at the beginning of 1970s. Bioactive fixation is defined as the "interfacial bonding of an implant to tissue by means of formation of a biologically active hydroxyapatite layer on the implant surface" [29]. These materials arose great expectations in the revolutionary period for medical care beginning just about 50 years ago. For centuries the problem of diseased or damaged body tissues had had little solution but the removal of the offending part. About 50 years ago transplantation or implantation became possible, but also implants made from biomaterials became available. These last had significant advantages over the first ones with regard to availability, reproducibility, and reliability. However they suffered problems of interfacial stability with host tissues and, obviously, lacked, with respect to living tissues, the ability to self-repair and to modify structure and properties in response to environmental factors such as mechanical load or blood flow.

The chapter is organized in four sections. The first one deals with synthesis and mechanism of formation of mesoporous bioactive glasses. The second one analyses the bioactive behavior. The third one is devoted to understand the specificity of bioactive response induced by the mesoporous structure. The fourth one deals with drug delivery from mesoporous bioactive glasses. In a first subparagraph the advantages of using bioactive glasses for local derivery and the construction of tissue engineering scaffolds are analysed. In the second one the complexity of therapeutics delivery from mesoporous bioactive glasses is analysed.

In order to improve orthopedic prostheses, lifetime special care was devoted to get better interfaces. Great attention was devoted to morphological fixation, exploiting large interface areas or fenestrations, or biological fixation, based on bone ingrowth, as alternative to cement fixation. Because of the ability to assure, after 3–6 months, a strength equal to or greater than the bone, bioactive bond to bone appeared to be a panacea for the interfacial stability problem. However at the end of the last century, it was recognized [29] that this is not true. The mismatch in mechanical properties at the bonded interface and the inability of the bioactive bonded interface to remodel in response to applied load have a detrimental effect on long-term interface stability [29]. Hench recognized [29] the need "to shift the emphasis of biomaterials research toward assisting or enhancing the body's own reparative capacity," that is, the need of a biomaterial that may enhance the regeneration of natural tissues, some kind of "regenerative allograft." He also very lucidly predicted that bioactive materials would keep on playing an outstanding role [29]. It is nowadays recognized that microporous and mesoporous inorganic and hybrid organic–inorganic bioactive matrices and scaffolds can be produced with controlled rates of resorption and controlled surface chemistries. The type and concentration of released inorganic and organic species and their release sequence can be tuned; this is a vital requirement in stimulating cell proliferation and enhancing subsequent cell differentiation [30, 34, 90]. The ability to bond to living tissues and the high pore

volume allow to exploit mesoporous bioactive materials also simply for local drug delivery allowing to overcome the limitations of systemic delivery: therapeutic concentrations at the site of infection but, for short periods of time, forcing repeated dosing for longer periods.

The chapter is organized in four sections. The first one deals with synthesis and mechanism of formation of mesoporous bioactive glasses. The second one analyzes the bioactive behavior. The third one is devoted to understand the specificity of bioactive response induced by the mesoporous structure. The fourth one deals with drug delivery from mesoporous bioactive glasses. In a first subparagraph, the advantages of using bioactive glasses for local delivery and the construction of tissue engineering scaffolds are analyzed. In the second one, the complexity of therapeutic delivery from mesoporous bioactive glasses is analyzed.

7.2 Mesoporous Bioactive Glasses (MBG)

According to the IUPAC definition [15], porous materials are divided into three classes: microporous (<2 nm), mesoporous (2–50 nm), and macroporous (>50 nm). Because of their high specific surface areas, porous solids were intensively studied [93] in the past for applications as adsorbents, catalysts, and catalyst support and, successively, in the field of sensors, drug delivery, and optical devices. A very great research activity was addressed [15] to zeolites that join good catalytic activity to the microporous structure. The relatively small pore openings however limited the range of their applicability. Porous glasses and gels do possess [15] larger pores, in the mesoporous dominion; however they show disordered pore system with broad pore size distributions. Intercalation of layered materials (double hydroxides, phosphates, and clays) gave also mesoporous solids with very broad mesopore size distributions.

MCM41 (Mobil Composition of Matter 41), discovered in 1992, was the first mesoporous solid possessing a regularly ordered pore arrangement and a very narrow pore size distribution [17, 48]. It can be produced in a wide range of experimental conditions exploiting interactions between silica and cationic surfactants. The strong adsorption of surfactant on the surface of silica particles had been, in earlier works, already exploited to control the flocculation of colloidal silica [39]. Moreover Iler in his book [40] reports on a patent of 1971 of V. Chiola et al. [14] assigned to Sylvania Electric Products Inc. in which “low bulk density silica” was described to be produced during hydrolysis and polycondensation of tetraethylorthosilicate (TEOS) in the presence of cationic surfactants. No other characterization than bulk density was reported in the patent. However, taking into account that when a surfactant is added to a soluble silicate MCM-41 is the more likely condensation product [17], the low density material of Chiola may be considered a forerunner of MCM-41 and also of surfactant template materials of different compositions [17, 35, 36].

7.2.1 Synthesis of Mesoporous Glasses

The production of mesoporous glasses exploits the templating action of surfactant molecules during the glass sol–gel synthesis. Generally speaking the sol–gel process is [3, 6] a synthesis route consisting in the preparation of a sol and successive gelation. Very popular precursors of the sol–gel synthesis of silicates are the metal-organic compounds like tetraethylorthosilicate (or tetraethoxysilane) $Si(OC_2H_5)_4$, shortly indicated with the acronym TEOS. A silicatic framework may be obtained through hydrolysis:

$$\equiv Si-OR + H_2O \leftrightarrow \equiv Si-OH + ROH$$

and polycondensation reactions:

$$\equiv Si-OR + HO-Si \equiv \leftrightarrow \equiv Si-O-Si \equiv + Si-OH$$

$$\equiv Si-OH + HO-Si \equiv \leftrightarrow \equiv Si-O-Si \equiv + H_2O$$

Polycondensation turns monomers into oligomers and, finally, inorganic polymers in the form of gels. The gels may then be converted to xerogels, glasses, and films. When the hydrolysis and polycondensation of alkoxysilicates occurs in basic (ammonia) alcoholic solutions (Stöber method), monodisperse particles from less than 0.05 to 2 μm may be easily obtained [3, 6, 94].

MCM 41 is the most popular product of the series M41S that may be obtained from solutions of tetraethylorthosilicate (TEOS), water, and cetyltrimethylammonium (CTMA) cation at 100 °C.

If the surfactant/silica molar ratio increased from 0.5 to 2, the siliceous products obtained were identified [102] and could be classified into four separate groups: MCM-41 (hexagonal), MCM-48 (cubic), thermally unstable M41S, and, a molecular species, the organic octamer $[(CTMA)SiO_{2.5}]_8$. One of the thermally unstable structures was identified as a lamellar phase. In Figs. 7.1 and 7.2, the structures of MCM41 (hexagonal) and MCM48 (cubic) are represented.

A liquid crystal templating mechanism was initially proposed. In Fig. 7.3 the schematic drawing of the liquid crystal templating mechanism initially proposed for MCM41 is shown. Hexagonal arrays of cylindrical micelles form (possibly mediated by the presence of silicate ions) with the polar groups of surfactant to the outside. In mechanism A silicate species then occupy the spaces between the cylinders. Alternatively (mechanism B) the silicate species generated in the reaction mixture influence the ordering of surfactant micelles. The final calcination step burns off the original organic material leaving hollow cylinders of inorganic material. The formation of hexagonal, cubic, or lamellar M41S structures by varying the silica concentration at constant surfactant concentration was considered [102] as a support for pathway B.

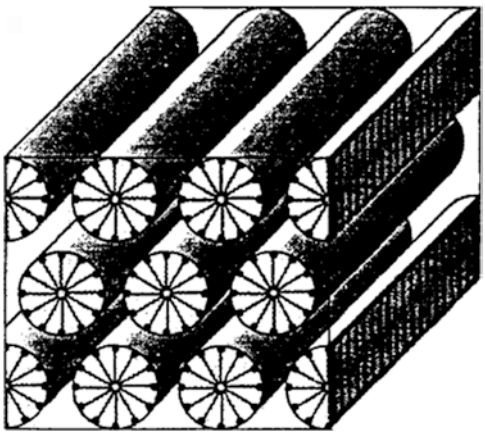

Fig. 7.1 Structure of MCM-41 (*hexagonal*) [92]

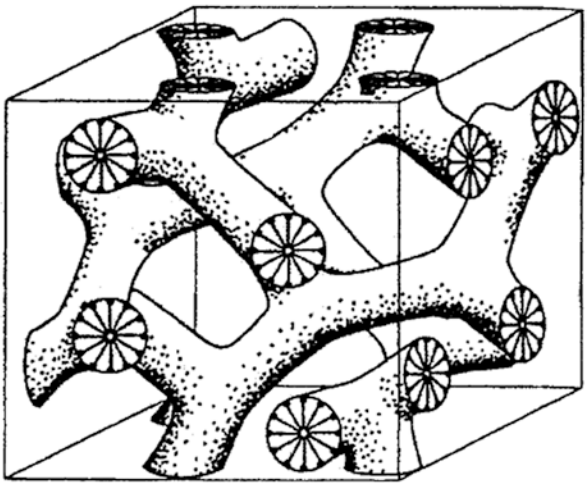

Fig. 7.2 Structure of MCM-48 (cubic) [92]

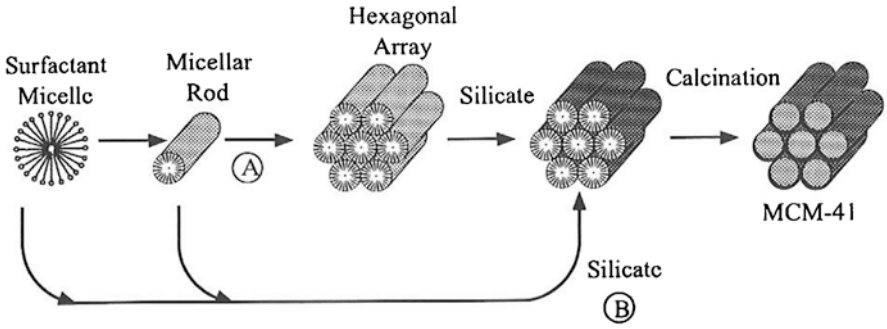

Fig. 7.3 Possible mechanistic pathways for the formation of MCM41: (**a**) Liquid crystal phase initiated; (**b**) silicate anions initiated [102]

However, M41S materials are limited to a pore diameter of approximately 80 Å, and, furthermore, they have significant external surface areas. These characteristics limit [48] their use in size-selective separations of large biomolecules such as proteins and enzymes.

Zhao et al. [117, 118] extended the family of highly ordered mesoporous silicates by synthesizing Santa Barbara Amorphous (SBA)-type materials. These have pore size ranging between 20 and 300 Å and use nonionic block copolymers as structure-directing agents in highly acidic media. SBA-15 raised particular interest [48]. It was synthesized using tri-block copolymer poly(ethylene oxide)–poly(propylene oxide)–poly(ethylene oxide), which is commercially available as pluronics P123 (EO20PO70EO20). SBA-15 possesses large BET surface area (>700 m^2/g), large pore diameter, and large pore wall thickness. The large wall thickness results in higher hydrothermal stability than M41S materials [117]. SBA-15 was synthesized as thin films [97], spheres [37, 54–57, 65, 96, 114, 120], fibers [8, 56, 57], and membranes [119]. It was also synthesized [48] as monodisperse, micrometer-sized (4–10 μm) spherical particles with large pore diameter (28–127 Å).

In the particle synthesis, parameters such as stirring rate, temperature, ionic strength, pH, and reactant composition so as the use of cosurfactants and swelling agents can influence the morphology of SBA-15 particles [48, 114]. In a typical synthesis [48], TEOS was added drop by drop to the surfactant solution; the mixture was vigorously stirred at 35 °C, stored at 75 °C, and finally aged in the range 80–125 °C. The surfactant solution was obtained by dissolving initially P123 into (1.5 M) HCl and successively adding the desired amount of aqueous solution of an ionic cosurfactant (cetyltrimethyl ammonium bromide (CTAB)) and a swelling agent (TMB, 1,3,5-trimethylbenzene). The addition of the swelling agent allowed [48] to obtain greater pore diameter and pore volume without change of surface area but gave pore size distribution more skewed and wider and could change the particle morphology from the spherical one. The presence of CTAB and TMB was important [48] to obtain spherical particles; however the yield of them decreased as the CTAB concentration was increased. This should be correlated to the role played by the ionic cosurfactant CTAB at level of the interaction between the surfactant and positively charged silica. The aging temperature also has influence [48]; its increase makes the pore size to grow and the microporosity to decrease.

New spherical silica nanoparticles with radial wrinkle structure (wrinkled silica nanoparticles (WSNs)) were recently synthesized [71, 81, 84, 116]. Their radial wrinkle structure which widens radially outward is expected to enhance the accessibility of functional materials inside their pores. They are obtained from oil-in-water macroemulsions within which droplets that are constituted of bicontinuous microemulsion are dispersed [71].

Recently a simple evaporation-induced self-assembly (EISA) process was proposed [7, 64, 78, 79] that enables a rapid production of patterned porous or nanocomposites materials in the form of films, fibers, and powders. It is based on the rapid evaporation of solutions of surfactants and pre-hydrolyzed alkoxysilanes. In a

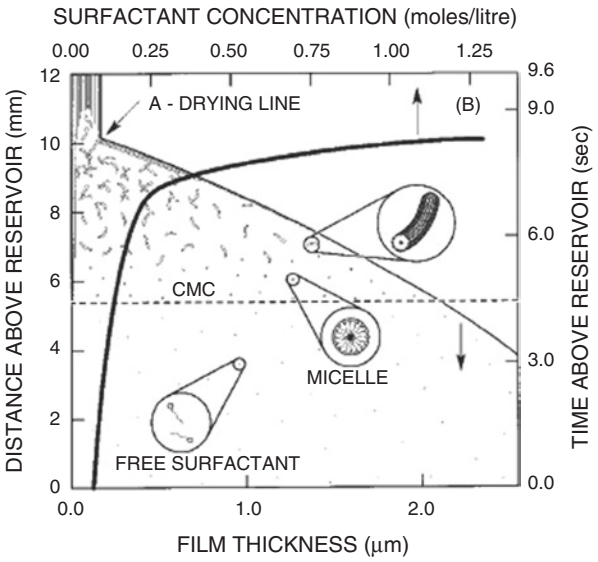

Fig. 7.4 Steady-state film cross section, showing changes in film thickness and composition (reported on the *horizontal axes*) as a function of distance above the sol reservoir surface and the corresponding time required for the substrate to move that distance (reported on the vertical axes) [64]

typical synthesis, films may be deposited on a substrate by dipcoating. Figure 7.4 shows the changes of both film thickness and concentration profiles [7, 64] as a function of distance above reservoir and time elapsed. It shows that, after a short time and at a short distance from the sol reservoir (about 8 s and 10 mm for the experiment reported in the figure), the film profile becomes steady, in correspondence of a thickness of about 0.2 μm. The initially homogeneous colloidal solution of silica and surfactant in ethanol/water solvent with a surfactant concentration less than the critical micelle concentration (cmc) is subjected to alcohol evaporation during drawing from the sol reservoir. The concentration of all species increases, but their ratio, in particular the surfactant/silica one, remains constant. So as schematically shown in Fig. 7.4, the progressively increasing surfactant concentration drives, above cmc, self-assembly of silica–surfactant micelles and their further organization into liquid crystalline mesophases. The silica–surfactant mesostructures present at solid–liquid and liquid–vapor interfaces at c<cmc serve to nucleate and orient mesophase development with respect to the substrate. Changes of initial alcohol/water/surfactant mole ratios reflect in different final mesostructures: hexagonal, cubic, and lamellar.

In a similar way (Brinker 1999), in the aerosol-assisted self-assembly, evaporation-induced self-assembly of liquid droplets allows to produce nanostructured particles with well-defined pore sizes and pore connectivities.

Mesoporous silica is bioactive. Recently bioactive glasses of more complex composition in the systems $CaO\text{-}SiO_2\text{-}P_2O_5$ and $SrO\text{-}SiO_2$ were successfully synthesized as highly ordered mesoporous ones by exploiting the surfactant templating route [34, 41, 107–109, 113]. They were obtained by adding calcium or strontium nitrate salts and, in the case of the ternary glass, triethyl phosphate to the surfactant/TEOS synthesis batch. In a typical synthesis the surfactant, TEOS, $Ca(NO_3)_2.4H_2O$, triethyl phosphate, and a solution 0.5 M HCl were dissolved, in due amounts, in ethanol and stirred at room temperature for 1 day. The resulting sol was introduced into a petri dish for an evaporation-induced self-assembly process, and then the dry gel was calcined at 700 °C for 5 h to obtain mesoporous bioactive glass powders. TEM micrograph reported in Fig. 7.5 shows that these mesoporous bioactive glass powders possess highly ordered one-dimensional channel structure with a pore size of 5 nm.

The mechanism of formation of mesoporous particles has been discussed in the literature with reference to silica particles. It is reported in the next paragraph.

7.2.2 Mechanism of Formation of Mesoporous Silica

Sometimes the mesoporous silica particles are in the nanometer size and do appear to contain hundreds of empty channels (mesopores) arranged in a 2D network of honeycomb-like porous structure so as can be seen in Figs. 7.1 and 7.5.

Recently more complex structures were reported ([60, 75, 82, 95, 96], Rankin 2004). In Fig. 7.6 the direct image of the internal structure of a mesoporous silica particle embedded in epoxy resin and sectioned using an electron beam is shown [75].

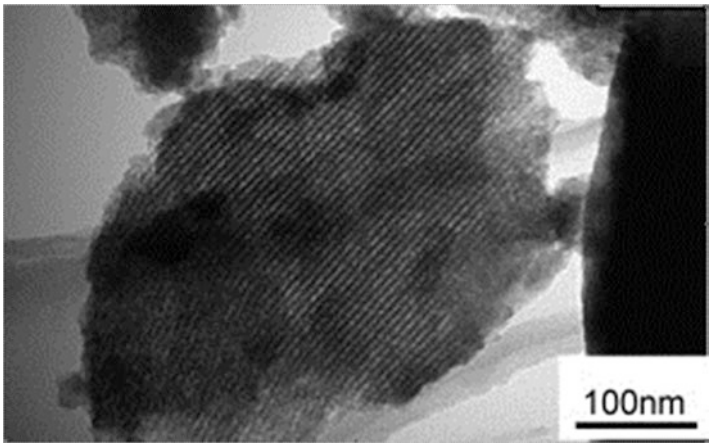

Fig. 7.5 TEM image of $CaO\text{-}SiO_2\text{-}P_2O_5$ mesoporous bioactive glass (Si/Ca/P ¼ 80/15/5) [107]

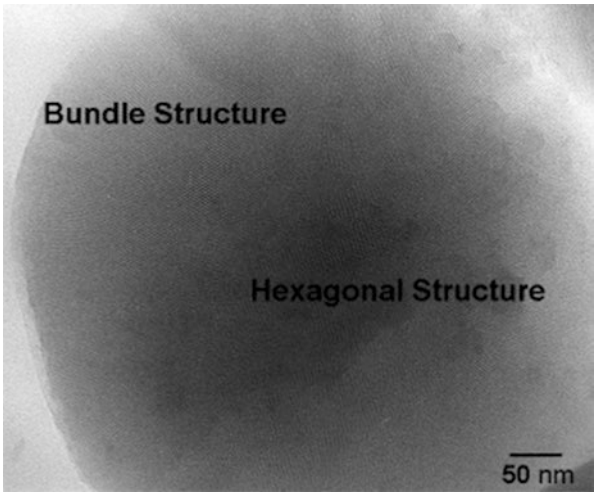

Fig. 7.6 Transmission electron micrograph (*TEM*) image of a sample embedded in an epoxy resin. The embedded sample was cut by an electron beam [75]

A structure consisting of bundled mesopores can be clearly seen near the surface of the hemisphere. Meanwhile, a hexagonal structure is observed at the center of the hemisphere, similar to the one shown in Figs. 7.1 and 7.5. The bundles of mesopores appear [75] to be aligned in three directions from the center to the surface of the particle. Meanwhile, radially aligned mesopores are observed on all surfaces of the growing particle. The mesopore alignment was followed during the course of the particle growth: it changed from three initial distinct directions to omnidirectional.

The development of uniform mesopores was first explained by a liquid crystal templating mechanism [58] and then by a cooperative templating mechanism [21, 35, 36]. Recently [75] a more complex mechanism was proposed to explain the formation of particles like the one shown in Fig. 7.6 that were obtained from tetramethylorthosilicate (TMOS) under basic conditions from methanol/water solutions, using hexadecyltrimethylammonium chloride (C16-TMACl) as the surfactant.

The mechanism of Nakamura [75] is represented in Fig. 7.7. The surfactant molecules are drawn as individual molecules rather than as micelles; this should be true as long as surfactant concentrations are less than the critical micelle concentration. Initially, hydrolyzed TMOS monomers condense to form oligomeric silica precursors through the reactions reminded in Sect. 7.2.1. However, when silica precursors attain a certain size by oligomerization, they are forced to precipitate as an organic–inorganic composite. In fact silica precursors contain a fair amount of silanols that dissociate to $Si\text{-}O^-$ and protons. In consequence, they are negatively charged. By contrast, surfactant heads have a positive charge. Therefore, silica precursors and surfactants can contact each other throughout the reaction. Upon certain size, the oligomeric silica structures, with surfactant molecules attached, assemble into small mesoporous silica particles with hexagonal regularity (of the type represented in Figs. 7.1 and 7.5), which then emerge from solution as primary particles. Any residual silica precursors then react preferentially with the surface silanols on the existing particles, eventually preventing the generation of new particles. It is not possible, however, that the particles grow by

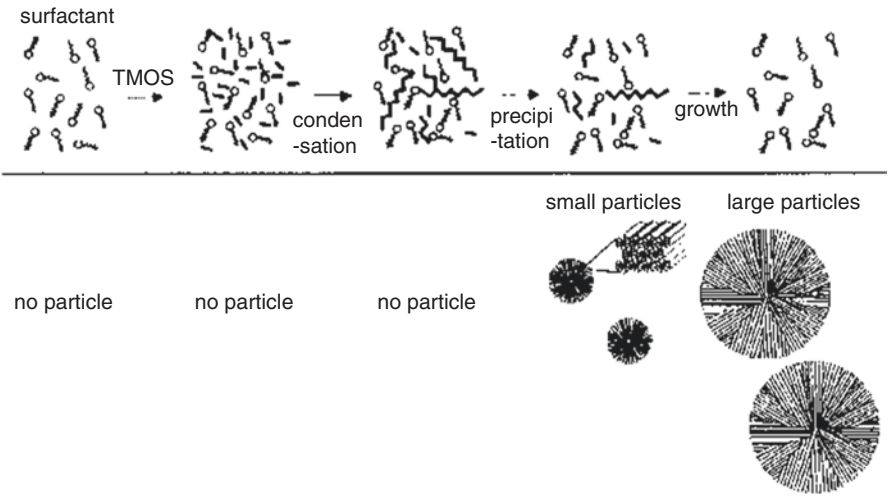

Fig. 7.7 Proposed mechanism for the formation of monodispersed mesoporous silica spheres. Progress of TMOS condensation is described above. Precipitation of particles is shown below. *Short lines* represent TMOS. *Zigzag lines* represent oligomeric TMOS [75]

the co-aggregation of smaller particles of the type represented in Figs. 7.1 and 7.5 (so as in the Stöber method). In this case the external "bundle structure" shown in Fig. 7.6 with mesopores aligned radially from the center to the surface of the particles and pointing in all directions could not be formed.

The mechanism proposed suggest that [75] the size of the particles could be enlarged by the addition of further TMOS. To confirm this, equimolar amounts of TMOS were added every hour for 4 h after the completion of the initial reaction (=1 h later). Figure 7.8 shows SEM images [75] of the particles that were obtained after two and four additions of TMOS to the initial reaction mixture. The diameters of the particles clearly increased upon the addition of TMOS while retaining their monodispersed characteristics (standard deviation are reported in parentheses). This result supports the notion that the additional TMOS would react preferentially with the surface silanol groups on the already formed particles rather than generating new particles and suggests a simple method to make the particles to grow. It was also shown [75] a method (hypothesized on the basis of the mechanism) to create monodispersed core/shell mesoporous silica spheres.

7.2.3 Mechanism of Formation of Mesoporous Silica When Using Two Immiscible Solvents (Wrinkled Particles)

Wrinkled particles may be obtained when two immiscible solvents are used. In a typical synthesis, 0.5 g (1.3 mmol) of cetylpyridinium bromide and 0.3 g (5.0 mmol) of urea were dissolved in 15 mL of water. Subsequently, 15 mL of cyclohexane and

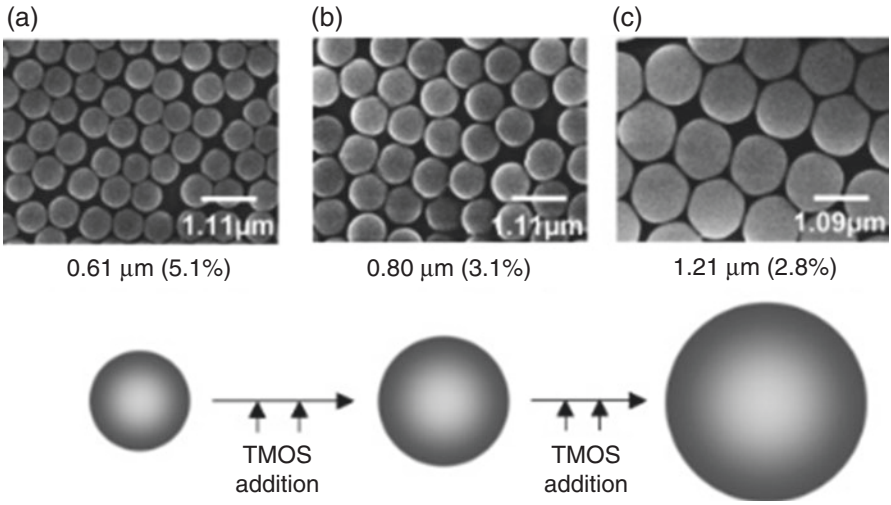

Fig. 7.8 SEM images of expanded particles obtained by the different TMOS addition times, (**a**) 0, (**b**) 2, and (**c**) 4, and schematic illustration of the particle growth. Standard deviations are in parentheses [75]

0.46 mL (6 mmol) of isopropanol is added to the solution. A two-phase system is obtained consisting of an upper microemulsion and a lower aqueous phase. Fast mechanical stirring gives an oil-in-water macroemulsion in which droplets, consisting of bicontinuous microemulsion, are dispersed [71]. With vigorous stirring, 1.25 g (6 mmol) of TEOS is added dropwise to the mixed solution. After vigorous stirring for 30 min at room temperature, the reaction mixture is heated up to 70 °C, and this state is maintained for 16 h.

The mechanism is represented in Fig. 7.9.

All reactions occur in the droplets that are, by themselves, bicontinuous microemulsions. TEOS dissolved in the oil layer comes into contact with the water at the emulsion interface where hydrolysis and condensation reactions occur. Ionized silicate monomers and oligomers have negative charges and bind to headgroups of cationic surfactants by the Coulomb interaction. As the condensation reaction proceeds, the amount of partially condensed silica tetrahedra (Q^3 = silica tetrahedra with three bridging oxygens and one non-bridging oxygen negatively charged) decreases and that of fully condensed (Q^4 = silica tetrahedra with four bridging oxygens) increases. As Q^4 silicates cannot be ionized, the total negative charge density of silicates decreases. In order to maintain charge balance, the number of silicate attached to a headgroup of surfactant with multidentate binding increases, and, consequently, the headgroup area of the surfactant increases. Accordingly, the curvature of the water−oil interface surrounded by surfactants increases to the positive direction. The interface can form closed structure such of spherical or cylindrical shapes. The aggregation of these surfactant–silicate particles leads to the formation of a repetitive mesophase. Finally, through water layers that are connected with ridges, newly formed mesophases are deposited on nanoparticle seeds, and the overall structure of nanoparticle assumes the wrinkle shape.

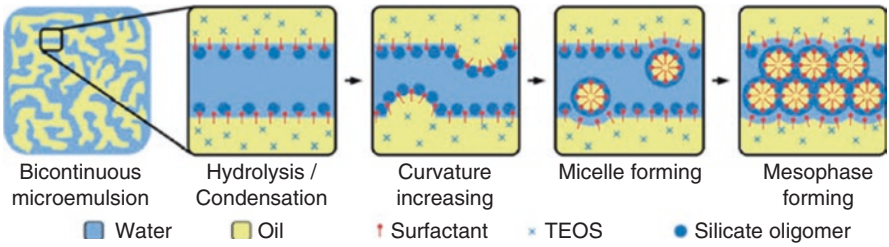

Fig. 7.9 Schematic illustration of the mesophase-forming mechanism from the microemulsion interface [71]

7.3 Bioactive Glasses

The first bioactive material was a glass obtained by quenching a melt of SiO_2 (45wt%), CaO (24.5wt%), Na_2O (24.5wt%), and P_2O_5 (6wt%), denoted bioglass 45S5. Successively [29, 33, 49, 53, 61, 83, 104] other compositions in the system SiO_2/CaO/P_2O_5 and in the quaternary system SiO_2/CaO/MgO/P_2O_5 at low P_2O_5 content were discovered to be bioactive. In Fig. 7.10 the compositional range of bioactive compositions in the ternary system SiO_2-CaO-P_2O_5 is reported. Figure 7.10 shows also that when produced through sol–gel method, the glasses were more bioactive, and the compositional range of bioactivity was extended till pure gel silica [29].

Figure 7.11 shows how good the interface between the bioactive glass and bone may be. It shows the SEM micrograph of the interface between the glass S46P0 and bone after 8 weeks in rabbit tibia [2]. SEM/EDX analysis shows that a continuous change of composition occurs at the interface from the glass to the bone one.

Bioactivity is the result of a complex process occurring at the surface of the glass [29]. The interaction [28, 30, 50, 51] is, at the beginning, due to the reactions between the glass and the blood plasma, which is an aqueous solution buffered at slightly basic pH = 7.2–7.4. The first five steps are:

1. First, the rapid exchange reaction of alkaline or alkaline earth ions with H^+ from solution:

$$\equiv SiO_2^- Ca^{2+} + 2H^+ \leftrightarrow 2SiOH + Ca^{2+}$$

It is well known in fact [86] that alkali or alkaline hearth silicate glasses in acidic or weakly alkaline (pH < 10) conditions are subjected to leaching of the less tightly bonded modifier cations (alkali or alkaline hearth ones) present in their composition

2. Loss of soluble silica in the form of $Si(OH)_4$ to the solution as the effect of hydrolysis reaction:

$$\equiv Si-O-Si\equiv + H_2O \leftrightarrow 2\equiv Si-OH$$

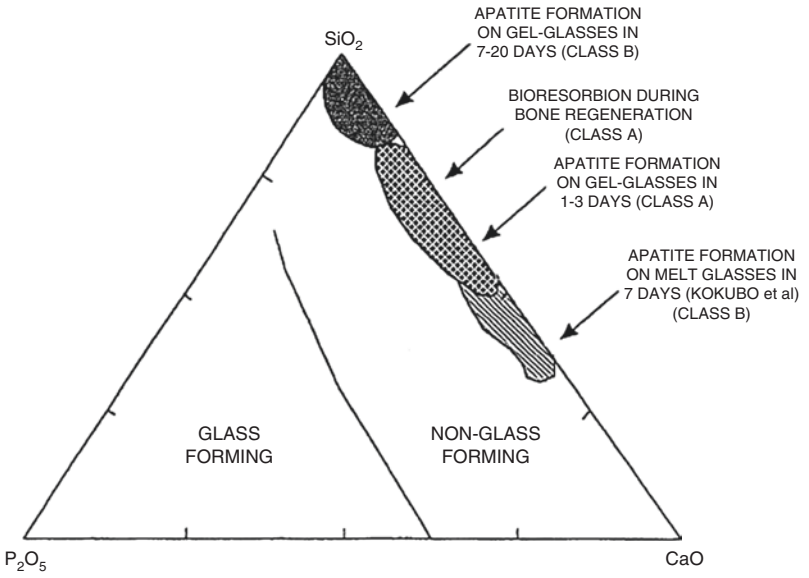

Fig. 7.10 Compositional range of bioactive gel glasses in the system $SiO_2/CaO/P_2O_5$ [29]

This may become possible as the result of pH increase in the reaction layer due to the occurrence of step 1

3. Condensation and repolymerization to form a gel SiO_2-rich layer on the surface depleted in the alkaline and alkaline earth cations:

$$\equiv Si-OH+HO-Si \equiv \leftrightarrow Si-O-Si+H_2O$$

In fact while some silica may be lost as the result of reactions described in step 2, some silanols groups may recondense giving a "gel" network, looser than the original one

4. Migration of Ca^{2+} ions to the surface through the gel SiO_2-rich layer and formation of an amorphous $CaO–P_2O_5$-rich film by precipitation from the supersaturated solution

$$\equiv Si-OH+HPO_4^{2-} \leftrightarrow \equiv Si-O-PO_3^{2-}+H_2O$$

5. Crystallization of the amorphous $CaO–P_2O_5$ film by incorporation of OH^- and/or CO_3^{2-} anions from solution to form a mixed hydroxyl carbonate apatite layer

The described steps give well account of the SEM/EDX results of Fig. 7.11 showing progressive changes of SiO_2, P_2O_5, and CaO concentrations at the bioactive glass/bone interface: a hydroxyl carbonate apatite (HCA) layer forms well anchored in the gel silica layer that forms trough degradation of glass surface. The behavior

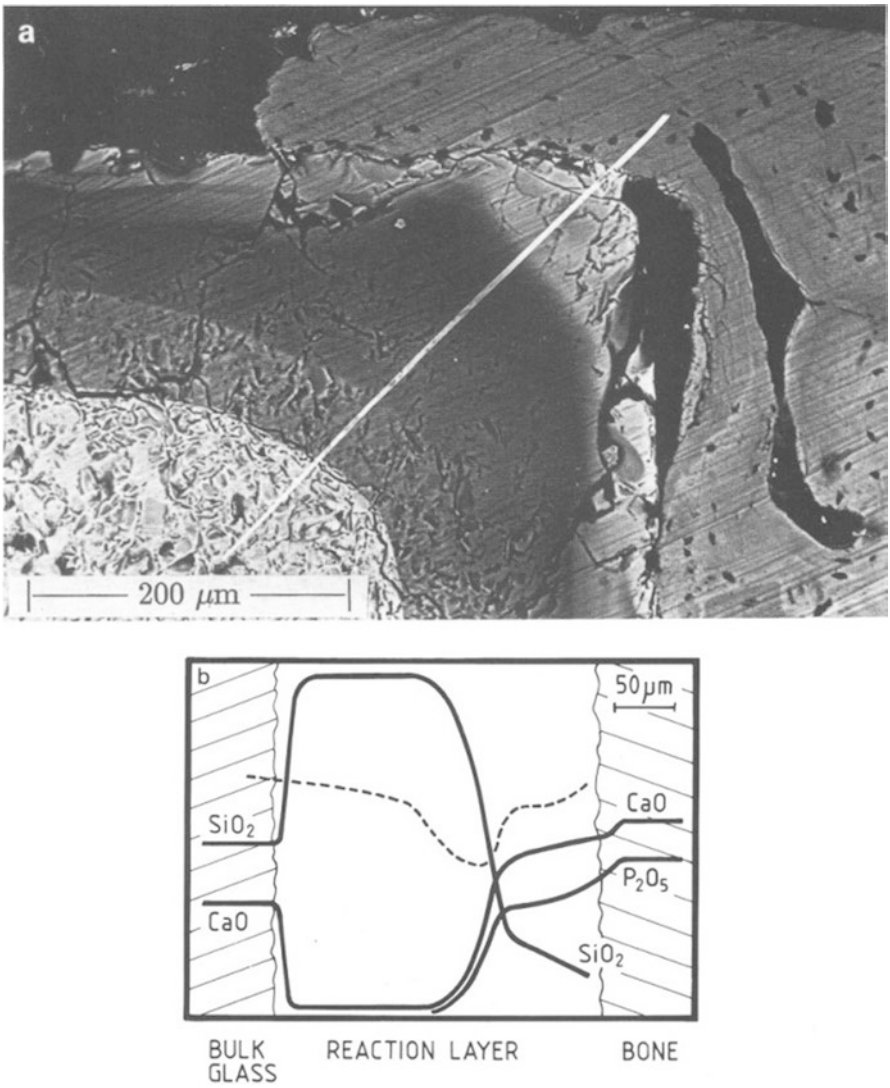

Fig. 7.11 Interface between the glass S46P0 and bone after 8 weeks in rabbit tibia [2]

strongly depends on the acidic character of silanol groups. When the glass composition is changed by addition of other components influencing the silanol acidity (like oxides of formula M_2O_3 where M = La, Y, In, Ga, Al), the ability to form a calcium phosphate layer is modified [4]. It is believed that the formed hydroxyl carbonate apatite is compositionally and structurally similar to the one present in the bone; this makes it biologically active and allows the following (6–11) steps to occur [29]:

6. Adsorption of biological moieties in HCA layer
7. Action of macrophages
8. Attachment of stem cells
9. Differentiation of stem cells
10. Generation of matrix
11. Crystallization of matrix

The formation of HCA layer is considered to be essential for the development of bioactivity. This allows to study bioactivity and to select bioactive compositions through an "in vitro" methodology allowing to remarkably reduce the number of animals used and the duration of animal experiments [52]. In fact in 1980, Hench et al. [80] had showed that an SiO_2-rich layer and calcium phosphate film form on the surface of bioglass when implanted in the body environment, which allows bonding to the living bone, and that the in vivo formation of the calcium phosphate film can be reproduced in a buffer solution consisting of Tris hydroxymethylaminomethane and hydrochloric acid (Tris buffer solution) at pH 7.4. In the early 1990s, Kokubo et al. proposed [52] to assess bioactivity by exposing the material to a protein-free acellular simulated body fluid (SBF) having pH and ionic composition very close to the blood plasma one and verifying the formation of HCA. The composition of SBF was successively revised and slightly corrected [52]. Good correlations were found between the in vitro and in vivo tests, and the "SBF method" was standardized as the solution for in vitro evaluation of apatite-forming ability of implant materials by the International Organization for Standardization (ISO 23317:2014). Many bioactive materials have been discovered [18, 83, 101]. They are distinguished in two classes [29]. Many exhibit only osteoconductivity [42], defined as the characteristic of bone growth and bonding along a surface (bioactive materials of class B). An example is constituted by synthetic hydroxyapatite. Class A bioactive materials are, instead, both osteoconductive than osteoproductive (also said osteoinductive). Osteoproduction is linked to enhanced mitosis and differentiation of osteoblast stem cells stimulated by slow resorption of the Class A bioactive particles [29]. Ionic products release from the glass play, therefore, a fundamental role. Some bioactive glasses are able to bond also to soft tissues [29]. The bioactivity of different materials may be compared [29] on the basis of the index of bioactivity $I_B = 100/t_{0.500}$, where $t_{0.500}$ is the time for 50% of the interface to be bonded to the bone.

7.4 Bioactivity of Mesoporous Glasses

Mesoporous silica produced through hydrolysis and polycondensation of alkoxysilanes is bioactive. Recently several more complex mesoporous bioactive glasses were produced [25, 34, 41, 43, 63, 90, 107–109, 113, 115].

Mesoporous glasses, also called template glasses, express accelerated bioactive response compared with conventional or sol–gel glasses of analogous composition [41, 90]. For example in the case of the mesoporous glass, S58 m (58% SiO_2–37%

$CaO – 5\%P_2O_5$) formation of calcium hydroxyapatite (HCA) occurs in 8 h, whereas in the correspondent sol–gel glass, its formation requires 3 days [41]. Moreover a greater amount of calcium phosphate is observed to form and crystallization of the initially amorphous phosphate layer occurs through formation of octacalcium phosphate (OCP) that successively transforms into the HCA crystalline phase, whereas HCA directly forms in the case of conventional and sol–gel glasses. These differences can be explained [41, 90] considering the higher values of specific surface area and pore volume of template glasses as well as the higher concentration of silanol (Si–OH) groups on the template glasses surface. The bioactivity mechanism, in fact, is similar to the one proposed in paragraph 7.3, except for some differences strictly linked to the compositional and structural differences reminded above. In fact, with reference to the mechanism reported in paragraph 7.3, we may expect and/or observe [41, 90] that:

(a) The exchange of Ca^{2+} in glass with H^+ in the solution (step 1 of the bioactivity mechanism) is quicker and produces a higher incorporation of H^+ ions and a higher density of silanols (Si–OH) groups.
(b) A highly protonated silica gel forms after the condensation of silanol groups (steps 1–3 of the mechanism), leading to an acid local pH (possibly pH = 6.7) on the glass surface.
(c) The precipitation of amorphous calcium phosphate (ACP) layer (step 4) is higher.
(d) The crystallization of ACP by incorporation of Ca^{2+} and HPO_4^{2-} leads to octacalcium phosphate (OCP) formation instead of carboxylate hydroxyapatite (HCA).
(e) OCP converts, later, into HCA through dehydration and hydrolysis reaction.

It is worth remembering that OCP is considered to be a precursor of carboxylate hydroxyapatite in the process of the tooth enamel, dentine, and bone formation in the living organisms. The formation, at first, of OCP instead of HCA (that directly forms in the case of the glasses obtained through melt quenching or sol–gel in the absence of surfactant) would occur [41, 90] because of the acidic character the surface of mesoporous bioactive glasses do possess when precipitation and crystallization of phosphate layer occurs. It is known in fact that OCP forms in acidic conditions. Therefore the process of formation of HCA in mesoporous bioactive glass (MBG) more closely resembles the one occurring in nature.

7.5 Drug Delivery from Mesoporous Bioactive Glasses

Because of their ability to bond to living tissues, bioactive glasses allow to exploit the approach of “local delivery” and overcome the problems connected also with systemic deliverable vectors [1, 34, 72]. In systemic delivery biomolecules can be inactivated by enzymes or chemical reactions in the blood, and so a relatively high concentration of drug is needed to provide sufficient dose at the desired location. These problems may be partly overcome with the use of vectors; some therapeutics may, however, be lost in other body compartments than the one they are

addressed to. Considerable research effort is therefore addressed [34, 90] to the topic of using bioactive glasses for the encapsulation, delivery, and controlled release of bioactive molecules and therapeutic drugs. Moreover, so as predicted by Hench [29], there is today a very great interest and research activity addressed to the use of bioactive glasses to produce scaffolds for tissue engineering [11, 13, 22, 23, 27, 44, 85]. Key properties like drug-delivery ability, biocompatibility, biodegradability, osteoconductivity, as well as osteogenic and angiogenic potential make them [34] excellent candidates for bone tissue scaffolds [76]. However a number of other strict requirements may be successfully satisfied by bioactive glasses so as described in the first subparagraph. The second paragraph is instead strictly related to the therapeutics release.

7.5.1 Bioactive Glasses for Local Drug Delivery and Tissue Engineering

Osteoporosis, fracture healing, defects filling, and spinal lesion reparation affect millions of people with a very big social cost [24]. The expectations from tissue engineering are great, particularly to overcome the problem of the shortage of living tissues and organs available for transplantation. Tissue engineering needs a scaffold that is a porous structure that must guide new tissue formation by supplying a matrix with interconnected porosity and tailored surface chemistry for cell growth and proliferation and the transport of nutrients and metabolic waste [24]. The scaffold should mimic the morphology, structure, and function of the bone in order to optimize integration with surrounding tissues. To do all this, the ideal scaffold should [24, 38]:

- Possess high three-dimensional interconnected porosity for cell growth, flow transport of nutrients, and metabolic waste and angiogenesis
- Be biocompatible and bioresorbable with a controllable degradation and resorption rate to match cell/tissue growth in vitro and/or in vivo
- Possess suitable surface chemistry for cell attachment, proliferation, and differentiation
- Possess mechanical properties (e.g., stiffness, strength, and fracture resistance) to match those of the tissues at the site of implantation

Concerning the first requirement, interconnected pores with a mean diameter (or width) of 100 μm or greater and open porosity of >50% are considered to be the minimum requirements to permit tissue ingrowth and function in porous scaffolds [23, 47]. It may be satisfied through one of the several well-established bioactive glass scaffold fabrication methods [23]:

- Sol–gel processing
- Thermal bonding of particles or fibers
- Polymer foam replication

- Solid freeform fabrication
- Freeze casting of suspensions

It is expected that by properly selecting composition and fabrication method, also the other above reminded requirements may be fulfilled.

When comparing the strength and elastic modulus of natural and synthetic materials (typically with a dense microstructure containing no porosity) [23, 105], it appears that the mechanical response of the bone is not matched by the biodegradable polymers, ceramics, or alloys currently used in orthopedic applications. Recently it was shown that, by optimizing the composition, processing and sintering conditions, bioactive glass scaffolds can be created with predesigned pore architectures and with strength comparable to human trabecular and cortical bones [22, 23, 62]. Moreover the compressive strengths of bioactive glass scaffolds strongly depend on composition and fabrication method [23]. In particular porous bioactive glass scaffolds can be fabricated with compressive strengths comparable to the values reported for human trabecular and cortical bones [23]. Toughening of bioactive glass scaffolds can be obtained through polymer coating. Biodegradable polymers, such as poly(D,L-lactic acid), PDLLA, poly(3-hydroxybutyrate), P(3HB), alginate, and PCL, have been used to coat bioactive glass scaffolds [5, 12, 23, 73]. The main energy dissipation mechanism was believed [23] to be polymeric fibril extension and crack bridging, so as in the bone which is a composite of hydroxyapatite and collagen.

The second requirement (biocompatibility and bioresorbability) may also be fulfilled if we take into account that, so as predicted by the bioactivity mechanisms reminded in Sects. 7.3 and 7.4, surface reactions leading to the bond formation of bioactive materials and living tissues start with a partial dissolution of the material surface. As a consequence bioactive materials may become bioresorbable when the sizes are reduced. It has been well demonstrated with bioglass particles. If small enough particles of a bioactive ceramic are used, the surface degradation may finally produce the total degradation of the particles [90]. Wilson and Noletti [90] found that particles of 100 μm in diameter of bioglass were resorbed or phagocytosed by macrophages in vivo, while larger particles were bioactive stimulating the bone growth. Schepers and Ducheyne [91] and Salinas and Vallet-Regı [87] indicated that particles under 300 μm in size were fully resorbed in vivo. Moreover a peculiar characteristic of the glasses is the lack of stoichiometric ratios of the chemical components: glass structures may be easily enriched with other components, in contents that may be largely changed and optimized with respect to the property required. Therefore the structure and chemistry of glasses can be tailored over a wide range, by changing either composition or thermal or environmental processing history, making possible to design glass scaffolds with variable degradation rates to match that of bone ingrowth and remodeling [23].

The requirement about surface chemistry for cell attachment, proliferation, and differentiation is treated in more detail in the paragraph 7.5.2.

7.5.2 *Release of Therapeutics from Mesoporous Bioactive Glasses*

It is recognized, from a long time, that a biologically relevant release of ionic products occurs from the surface of bioactive glasses. They may induce angiogenesis in addition to influencing gene expression and promoting osteoblastic differentiation. In addition therapeutic drugs or biologically active molecules may be easily introduced. Owing to their high pore volume, mesoporous bioactive glasses offer, in this respect, additional exceptional opportunities. In the following these three topics will be better addressed. The first two subparagraphs refer generally to bioactive glasses. The third one shows the additional great opportunities linked to the mesoporous structure.

7.5.2.1 Ionic Dissolution Products from Bioactive Glasses

Recently, the ionic dissolution products from bioglass (e.g., Si, Ca, P) and from other silicate-based glasses were shown to stimulate expression of several genes of osteoblastic cells and angiogenesis in vitro and in vivo, while possible antibacterial and inflammatory effects of bioactive glasses have also been investigated [31, 34].

A schematic overview of biological responses to ionic dissolution products of bioactive glasses is given in Fig. 7.12. Table 7.1 gives a summary of biological

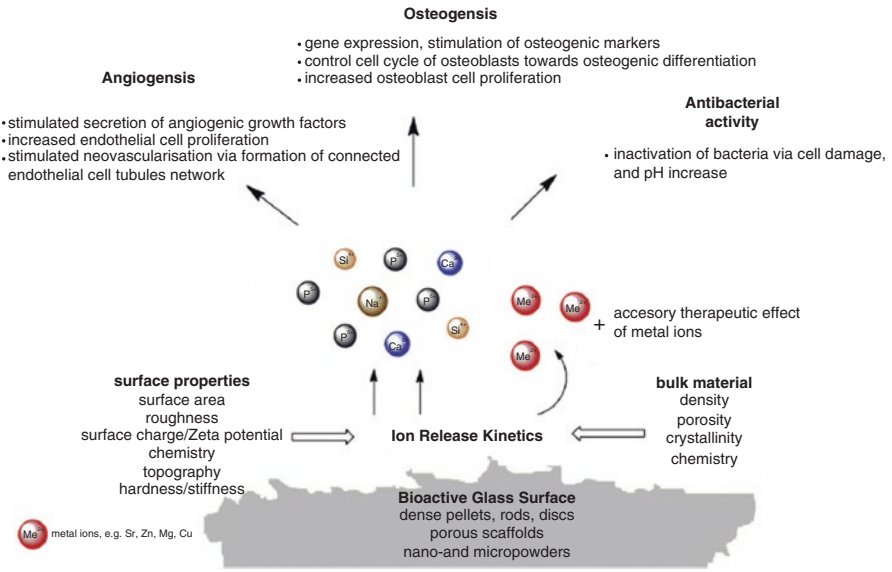

Fig. 7.12 Overview of biological responses to ionic dissolution products of bioactive glasses [31]

Table 7.1 Effect of selected metallic ions on human bone metabolism and angiogenesis: summary of literature studies [31]

	Biological response in vivo/in vitro	Reference
Si	Essential for metabolic processes, formation, and calcification of bone tissue	[9, 10]
	Dietary intake of Si increases bone mineral density (BMD)	[45]
	Aqueous Si induces hydroxyapatite (HAp) precipitation	[16]
	$Si(OH)_4$ stimulates collagen I formation and osteoblastic differentiation	[87]
Ca	Favors osteoblast proliferation, differentiation, and extracellular matrix (ECM) mineralization	[66]
	Activates Ca-sensing receptors in osteoblast cells and increases expression of growth factors, e.g., IGF-I or IGF-II	[69, 100]
P	Stimulates expression of matrix gla protein (MGP) a key regulator in bone formation	[46]
Zn	Shows anti-inflammatory effect and stimulates bone formation in vitro by activation protein synthesis in osteoblasts	[111]
	Increases ATPase activity and regulates transcription of osteoblastic differentiation genes, e.g., collagen I, ALP, osteopontin, and osteocalcin	[59]
Mg	Stimulates new bone formation	[121]
	Increases bone cell adhesion and stability (probably due to interactions with integrins)	[121, 112]
Sr	Shows beneficial effects on bone cells and bone formation in vivo	[69, 67]
	Promising agent for treating osteoporosis	[70]
Cu	Significant amounts of cellular Cu are found in human endothelial cells when undergoing angiogenesis	[20]
	Promotes synergetic stimulating effects on angiogenesis when associated with angiogenic growth factor FGF-2	[26]
	Stimulates proliferation of human endothelial cells	[32]
	Induces differentiation of mesenchymal cells toward the osteogenic lineage	[88]
B	Stimulates RNA synthesis in fibroblast cells	[77, 19]
	Dietary boron stimulates bone formation	[99]

responses to single inorganic species. Some ionic species (Ca, Si, P...) are usually present because bioactive glasses are often calcium phosphosilicate; the presence of other species (like Zn and Mg ions) may be assured by adding their oxides to the batch. Glasses, in fact, have not stoichiometric composition; this last may be widely and continuously changed like the composition of a solution.

Unfortunately the exact mechanism of interaction between the ionic dissolution products of such inorganic materials and human cells is not yet fully understood. Of course the favorable effects are expressed in correspondence of specific extracellular matrix compositions. These topics are nowadays actively investigated [31]. The release rates are a function of the glass surface and bulk properties so as indicated in Fig. 7.12. Producing glasses with tailored ion release kinetics and controlled biological response in the relevant physiological environment is expected to be successfully performed in the near future.

7.5.2.2 Therapeutic Drug or Biologically Active Molecule Release from Bioactive Glasses

An effective drug-delivery system should assure a controlled release of carried drug molecules in active form. Small molecule therapeutic drugs may cause, in fact, unwanted adverse events and systemic toxicity so as described and studied by pharmacokinetics (PK), determining the fate of substances administered to a living organism, and pharmacodynamics (PD), studying how the drug affects the organism. A therapeutic index is defined:

$$TI = LD_{50} / ED_{50}$$

where LD_{50} is the dose lethal in 50% of subjects and ED_{50} is the dose efficacious in 50% of subjects. Other adverse factors in systemic delivery are low aqueous solubility due to drug hydrophobicity, rapid clearance and extensive metabolism of the drugs in vivo, and nonspecific tissue accumulation. All these problems may be solved with the use of drug-delivery platforms. A very great interest is nowadays addressed to the bioactive glasses, especially the mesoporous ones, for the possibility they offer to have local delivery. The synthesis of them through sol–gel chemistry appears particularly valuable because it can be performed at room temperature. Therefore proteins, drugs, or other bioactive molecules can be incorporated by adding them directly to the synthesis batch since room temperature processing preserves their functionality. Another approach is soaking bioactive glass samples (eventually produced through melt quenching) in a solution of the desired loading molecule, which can be entrapped inside pores with or without chemical bonding . It's worth reminding, in fact, that molecules can be physically adsorbed on the pore or external glass surfaces; alternatively chemical bonding can be accomplished by the interaction of hydroxyl and amino groups of the molecules with the Si–OH groups and P-OH groups present on the bioactive glass surface.

Sol–gel bioactive glasses were successfully charged with antibiotics added to the initial alkoxide solution [34]. This is an important topic: antibiotics may avoid the consequences associated with the application of bone-filling materials, orthopedic implants, or bone replacements, inflammatory response or infections, e.g., osteomyelitis. A good example of the other approach is reported for melt-derived borate glass powders of composition $6Na_2O–8K_2O–8MgO–22CaO–54B_2O_3–2P_2O_5$ mol%. They were added [34] to a phosphate-buffered solution (PBS) with 80 mg/g vancomycin. The mixture was placed into rubber molds without compression and dried for 24 h, forming pellets which were ready to use. In vivo results showed that these borate glass delivery systems were effective in the treatment of chronic osteomyelitis in rabbits.

Bone morphogenetic proteins (BMPs), especially recombinant human BMP (rhBMP), are the main growth factors playing an important role in bone regeneration and in tissue engineering. Their addition should enhance [34] the bone regeneration capability of scaffolds leading to successful healing of critical bone defects. These proteins may be added to bioactive glasses in the above described manners. An example was documented by Tolli (2016) [98]. Different amounts of reindeer

bone extract (till 40 mg) were added to carboxymethyl cellulose (CMC) to form a gel that was combined with granules of bioactive glass S53P4 (composition of 53% SiO_2, 23% Na_2O, 20% CaO, and 4% P_2O_5 in wt%) at a ratio of 40:60wt%, shaped into rods with diameter of 5 mm and lyophilized. Bone proteins were expected to adhere to the surface of the bioactive glass granules and released upon bioactive glass dissolution. A beneficial effect of these composite implants in filling rabbit tibia defects was documented [98].

7.5.2.3 Drug Release from Mesoporous Bioactive Glasses

Enhanced in vitro and in vivo drug-delivery properties of mesoporous bioactive glasses (MBG) with respect to the non-mesoporous ones were well proved [34, 107–109]. This can be correlated, first of all, with the greater pore volume of MBG. A correlation, sometimes of direct proportionality, between the efficiency of drug loading and the pore volume of the material was found [34].

Drug molecules can be easily incorporated within the mesopores using the immersion technique. The drug release pattern is influenced by the pore diameter. It's worth remembering in fact that there are four different states of molecules hosted in MBG [34, 110]:

1. Molecules lying at the window of the mesopore
2. Molecules entrapped inside the mesopore without bonding
3. Molecules entrapped in the mesopore with bonding
4. Molecules adsorbed on the external MBG surface

As a consequence three drug release behaviors may be detected [34, 110]:

(a) An initial fast release rate due to molecules in the state described at points 1 and 4
(b) A reduced rate when molecules in the state 2 are released
(c) A final release stage, with an even more reduced rate, involving molecules in the state 3

A marked influence of the pore diameter is observed on the transition from regime b to c. In fact when reducing the pore diameter, the pore-specific surface (ratio of surface to volume of the pore) increases; the result is that the proportion of molecules entrapped in the mesopore with bonding (type 3) increases with respect to the nonbonded ones (type 2) with the consequent effects on the duration and relative relevance of stages b and c.

Taking into account that the bonding within the mesopores is accomplished due to the interaction of the hydroxyl and amino groups of the biomolecules with the Si–OH groups and P-OH groups in MBG, the effects of pH may be predicted. In fact the changes with pH of the silanol groups protonation and deprotonation equilibrium ($Si\text{-}O\text{-}H \Leftrightarrow Si\text{-}O^- + H^+$) make the interaction with biomolecules to change.

Recently on-demand release processes (also termed "switch on/off") were proposed which, in principle, allow tailored release profiles with excellent spatial, temporal, and dosage control [74, 103]. On-demand drug delivery is becoming feasible

through the design of stimuli-responsive systems that recognize their microenvironment and react in a dynamic way, mimicking the responsiveness of living organisms.

The literature relative to nanodelivery systems that carry therapeutic molecules attached through covalent linkers ("conjugated") was recently thoroughly and smartly reviewed [106]. It was recognized that there are numerous mechanisms of drug release via linker cleavage [74, 106]: ester, amide, or hydrazone hydrolysis, disulfide exchange, hypoxia activation, Mannich base, self-immolation, photochemistry, thermolysis, and azo reduction. The conditions that control drug release by triggering linker cleavage involve [74, 106] pathophysiological features and subcellular properties specific to diseased cells. Triggering mechanisms [74, 106] include tumor hypoxia (low oxygen levels due to increased metabolic rates in tumor cells), low intracellular pH (endosomes and lysosomes where targeted nanomaterials are taken up), lowered extracellular pH for tumor cells, tumor-specific enzymes (matrix metalloproteinase, prostate-specific membrane antigen) overexpressed on the cell membrane, and upregulation of glutathione.

Extracorporeal physical stimuli can be also applied. Sustained drug release can also be achieved by thermo-, magnetic-, light- or ultrasound-sensitive nanoparticulate systems.

The stimuli-responsive approach takes advantage of the existence of a great number of commercially available organoalkoxysilane molecules that allow easy surface functionalization of silica and silicates. The most popular one is aminopropyltrietoxysilane (APTS): $(C_2H_5O)_3Si(CH_2)_3NH_2$. The hydrolysis of the three ethoxy groups to silanol (Si-O-H) allows this molecule to graft to silica surfaces through condensation with silanols therein present. The non-hydrolyzable group linked through Si-C bond (in the case of APTS, the aminopropyl one) remains therefore exposed on the silica surface. This is a simple functionalizing process that allows to have at the surface of silica a great number of reactive groups. Examples of alternative commercially available organoalkoxysilane molecules are:

- Vinyltriethoxysilane: $CH_2=CHSi(C_2H_5O)_3$
- 3-(Trimethoxysilyl)propyl methacrylate: $H_2C=C(CH_3)CO_2(CH_2)_3Si(OCH_3)_3$
- 3-Glycidoxypropyltrimethoxysilane: $CH_2(O)CHCH_2O(CH_2)_3Si(OCH_3)_3$

As an example, a smart application of these concepts exploits [89] the low melting temperature of a nucleic acid duplex and the ability of superparamagnetic nanocrystals covalently linked to a nucleic acid strand to capture external electromagnetic energy: the energy released under an alternating magnetic field allows to break the hydrogen bonding pattern with its complementary strand. To do this, oligonucleotide-modified mesoporous silica, encapsulating magnetite superparamagnetic nanoparticles, was capped with magnetic nanocrystals functionalized with the complementary strand. The chosen DNA duplex had a melting temperature of 47 °C, which corresponds to the upper limit of therapeutic magnetic hyperthermia. Magnetite nanoparticles, produced through the Massart method and surface functionalized with APTS, were incorporated into mesoporous silica matrices by simply adding them to the synthesis reaction batch of silica. These magnetic silica particles were surface aminated through reaction with APTS. The oligonucleotide was anchored to

the aminated surfaces with the aid of a sulfo-SMCC linker (sulfosuccinimidyl-4-[N-aleimidomethyl]cyclohexane-1-carboxylate); 4-(N-maleimidomethyl)cyclohexane-1-carboxylic acid-3-sulfo-N-hydroxysuccinimide ester). The magnetic component of the whole system allowed reaching hyperthermic temperatures (42–47 °C) under an alternating magnetic field. Progressive double-stranded DNA melting, as a result of temperature increase, gave rise to uncapping and the subsequent release of a mesopore filling model drug, fluorescein. This example is a smart application in which magnetic and thermal stimuli-responsive materials are coupled to have a remote-controlled release of drug from mesoporous materials.

Other examples are reported in the literature [74, 89, 106].

7.6 Conclusions

Recently mesoporous bioactive glasses were synthesized for which outstanding applications in the biomedical field are expected.

The coupling of bioactivity to mesoporous structure allows local drug-delivery applications. The structure and chemistry of glasses can be tailored over a wide range, by changing either composition or thermal or environmental processing history, making possible to design glass scaffolds that match the requirements of porosity, bioresorbability, mechanical properties, and surface chemistry for cell attachment, proliferation, and differentiation.

The delivery of therapeutics is complex and offers unique perspectives. Bioactive glasses degrade by releasing ionic species of different types able to activate relevant biological responses that span from the stimulation of expression of several genes to angiogenesis and antibacterial effects. Some ionic species (Ca, Si, P...) are usually present because bioactive glasses are often calcium phosphosilicate; the presence of other species (like Zn and Mg ions) may be assured by adding their oxides to the batch. Glasses, in fact, have not stoichiometric composition; this last may be widely and continuously changed like the composition of a solution. Antibiotics and proteins may be easily added to bioactive glasses through soaking techniques. When using the sol–gel synthesis, they can be directly added to the synthesis reaction batch, thanks to the low synthesis temperatures at which their functionalities are preserved.

Enhanced in vitro and in vivo drug-delivery properties are recorded in the case of bioactive glasses possessing mesoporous structure, thanks to their high pore volume and possibility of modulating pore size. High pore volumes assure high payloads. The release kinetics are sensitive to the pore size. Finally mesoporous glasses may be easily surface functionalized. This makes possible to design “switch on/off’” release platforms.

References

1. Allen TM, Cullis PR. Drug delivery systems: entering the mainstream. Science. 2004; 303(5665):1818–22.
2. Andersson OH, Karlsson KH, Kangasniemi K. Calcium phosphate formation at the surface of bioactive glass in vivo. J Non Cryst Solids. 1990;119:290–6.
3. Branda F. The Sol-Gel route to nanocomposites. In: Boreddy SR, editor. Advances in nanocomposites – synthesis, characterization and industrial applications. Reddy, INTECH open access publisher; 2011. Available online: (http://www.intechopen.com/articles/show/title/the-sol-gel-route-to-nanocomposites).
4. Branda F, Arcobello-Varlese F, Costantini A, Luciani G. Effect of the substitution of M_2O_3 (M=La,Y,In,Ga,Al) for CaO on the bioactivity of 2.5CaO _ $2SiO_2$ glass. Biomaterials. 2002; 23:711–6.
5. Bretcanu O, Misra S, Roy I, Renghini C, Fiori F, Boccaccini AR, Salih V. In vitro biocompatibility of 45S5 bioglass-derived glass–ceramic scaffolds coated with poly(3-hydroxybutyrate). J Tissue Eng Regen Med. 2009;3:139–48.
6. Brinker CJ, Sherer W. Sol-gel science: the physics and chemistry of Sol-gel processing. San Diego: Academic Press; 1990.
7. Brinker JC, Lu Y, Sellinger A, Fan H. Evaporation-induced self-assembly: nanostructures made easy. Adv. Mater. 1999;11(7):579–85.
8. Bruinsma PJ, Kim AY, Liu J, Baskaran S. Chem Mater. 1997;9:2507.
9. Carlisle EM. Silicon: a possible factor in bone calcification. Science. 1970;167(3916):279–80.
10. Carlisle E. Silicon: a requirement in bone formation independent of vitamin D1. Calcif Tissue Int. 1981;33(1):27–34.
11. Chatzistavrou X, Tsigkou O, Amin HD, Paraskevopoulos KM, Salih V, Boccaccini AR. Sol–gel based fabrication and characterization of new bioactive glass–ceramic composites for dental applications. J Eur Ceram Soc. 2012;32:3051.
12. Chen QZ, Boccaccini AR. Poly(D,L-lactic acid) coated 45S5 bioglass®-based scaffolds: processing and characterization. J Biomed Mater Res A. 2006;77A:445–57.
13. Chen Q, Roether JA, Boccaccini AR. Chapter 6: Tissue engineering scaffolds from bioactive glass and composite materials. In: Ashammakhi N, Reis R, Chiellini F, editors. Topics in tissue engineering, vol. 4. 2008. http://www.oulu.fi/spareparts/ebook_topics_in_t_e_vol4/
14. Chiola V, Ritsko JE, Vanderpool CD, US Patent 3556725, 1971.
15. Ciesla U, Schüth F. Ordered mesoporous materials – review. Microporous Mesoporous Mater. 1999;27:131–49.
16. Damen JJM, Ten Cate JM. Silica-induced precipitation of calcium phosphate in the presence of inhibitors of hydroxyapatite formation. J Dent Res. 1992;71(3):453–7.
17. Di Renzo F, Cambon H, Dudartre R. A 28 years old synthesis of micelle templated mesoporous silica. Microporous Mater. 1997;10:283–6.
18. Duchène P. Stimulation of biological function with bioactive glass. MRS Bull. 1998;23(11): 43–9.
19. Dzondo-Gadet M, Mayap-Nzietchueng R, Hess K, Nabet P, Belleville F, Dousset B. Action of boron at the molecular level. Biol Trace Elem Res. 2002;85(1):23–33.
20. Finney L, Vogt S, Fukai T, Glesne D. Copper and angiogenesis: unraveling a relationship key to cancer progression. Clin Exp Pharmacol Physiol. 2009;36(1):88–94.
21. Firouzi A, Kumar D, Bull LM, Besier T, Sieger P, Huo Q, Walker SA, Zasadzinki JA, Glinka C, Nicol J, Margolese D, Stucky GD, Chmelka BF. Science. 1995;267:1138.
22. Fu Q, Saiz E, Tomsia AP. Bioinspired strong and highly porous glass scaffolds. Adv Funct Mater. 2011;21:1058–63.
23. Fu Q, Saiz E, Rahaman MN, Tomsia AP. Bioactive glass scaffolds for bone tissue engineering: state of the art and future perspectives. Mater Sci Eng C. 2011;31:1245–56.
24. Fu Q, Saiz E, Tomsia AP. Direct ink writing of highly porous and strong glass scaffolds for load-bearing bone defects repair and re generation. Acta Biomater. 2011;7:3547–54.

25. Garcıa A, Cicuéndez M, Izquierdo-Barba I, Arcos D, Vallet-Régı M. Essential role of calcium phosphate heterogeneities in 2D-hexagonal and 3D-cubic SiO_2-CaO-P_2O_5 mesoporous bioactive glasses. Chem Mater. 2009;21:5474–84.
26. Gérard C, Bordeleau L-J, Barralet J, Doillon CJ. The stimulation of angiogenesis and collagen deposition by copper. Biomaterials. 2010;31(5):824–31.
27. Gerhardt LC, Boccaccini AR. Bioactive glass and glass-ceramic scaffolds for bone tissue engineering. Materials. 2010;3:3867–910.
28. Hench LL. Bioceramics: from concept to clinic. J Am Ceram Soc. 1991;74(7):1487–510.
29. Hench LL. Biomaterials: a forecast for the future. Biomaterials. 1998;19:1419–23.
30. Hench LL, Splint RJ, Allen WC, Greenlee TK. Bonding mechanism at the interface of ceramic prosthetic materials. J Biomed Mater Res Symp. 1971;2(Part 1):117–41.
31. Hoppe A, Güldal NS, Boccaccini AR. A review of the biological response to ionic dissolution products from bioactive glasses and glass-ceramics. Biomaterials. 2011;32:2757–74.
32. Hu GF. Copper stimulates proliferation of human endothelial cells under culture. J Cell Biochem. 1998;69(3):326–35.
33. Hulbert SF, Young FA, Mathews RS, Klawitter JJ, Talbert CD, Stelling FH. Potential of ceramic materials as permanently implantable skeletal prosthesis. J Biomed Mater Res. 1970;4:433–56.
34. Hum J, Boccaccini AR. Bioactive glasses as carriers for bioactive molecules and therapeutic drugs: a review. J Mater Sci Mater Med. 2012;23:2317–33.
35. Huo Q, Margolese DI, Clesia U, Feng P, Gier TE, Sieger P, Leon R, Petroff PM, Schüth F, Stucky GD. Generalized synthesis of periodic surfactant/inorganic composite materials. Nature. 1994a;368:317–21.
36. Huo Q, Margolese DI, Ciesra U, Feng P, Gier TE, Sieger P, Firouzi A, Chmelka BF, Schuth F, Stucky GD. Organization of organic molecules with inorganic molecular species into nanocomposite biphase arrays. Chem Mater. 1994b;6:1176–91.
37. Huo Q, Feng J, Schüth F, Stucky GD. Preparation of hard mesoporous silica spheres. Chem Mater. 1997;9:14–7.
38. Hutmacher DW. Scaffolds in tissue engineering bone and cartilage. Biomaterials. 2000; 21:2529–43.
39. Iler RK, US Patent 2663650, 1953.
40. Iler RK. The chemistry of silica. New York: Wiley; 1971. p. 562.
41. Izquierdo-Barba I, Arcos D, Sakamoto Y, Terasaki O, Lopez-Noriega A, Vallet-Régı M. High-performance mesoporous bioceramics mimicking bone mineralization. Chem Mater. 2008; 20:3191–8.
42. Jarcho M, Bolen CH, Thomas MB, Bobick J, Kayand JF, Doremus RH. Hydroxylapatite synthesis and characterization in dense polycrystalline form. J Mater Sci. 1976;11:2027.
43. Jones JR. Review of bioactive glass: from Hench to hybrids. Acta Biomater. 2013;9:4457–86.
44. Jones JR, Ehrenfried LM, Hench LL. Optimising bioactive glass scaffolds for bone tissue engineering. Biomaterials. 2006;27:964–73.
45. Jugdaohsingh R, Tucker KL, Qiao N, Cupples LA, Kiel DP, Powell JJ. Dietary silicon intake is positively associated with bone mineral density in men and premenopausal women of the Framingham offspring cohort. J Bone Miner Res. 2004;19(2):297–307.
46. Julien M, Khoshniat S, Lacreusette A, Gatius M, Bozec A, Wagner EF, Wittrant Y, Masson M, Weiss P, Beck L, Magne D, Guicheux J. Phosphate-dependent regulation of MGP in osteoblasts: role of ERK1/2 and Fra-1. J Bone Miner Res. 2009;24(11):1856–68.
47. Karageorgiou V, Kaplan D. Porosity of 3D biomaterial scaffolds and osteogenesis. Biomaterials. 2005;26:5474–91.
48. Katiyar A, Yadav S, Smirniotis PG, Pinto NG. Synthesis of ordered large pore SBA-15 spherical particles for adsorption of biomolecules. J Chromatogr A. 2006;1122:13–20.
49. Klein C, Patka P, der Hollander W. Macroporous calcium phosphate bioceramics in dog femora: a histological study of interface and biodegradation. Biomaterials. 1989;10:59–62.
50. Kokubo T. Surface chemistry of bioactive glass-ceramics. J Non Cryst Solids. 1990;120: 138–51.

51. Kokubo T. Novel bioactive materials derived from glasses, proceedings of the XVI international congress on glass, Madrid, vol. 1. Bol Soc Esp Ceram Vid. 1992;31-C(1):119–37.
52. Kokubo T, Takadama H. How useful is SBF in predicting in vivo bone bioactivity? Biomaterials. 2006;27:2907–15.
53. Kokubo T, Ito S, Shigematsu M, Sakka S, Yamamuro T. Mechanical properties of a new type of apatite-containing glass-ceramic for prosthetic application. J Mater Sci. 1985;20:2001–4.
54. Kosuge K, Singh PS. Rapid synthesis of Al-containing mesoporous silica hard spheres of 30-50 μm diameter. Chem Mater. 2001;13:2476–82.
55. Kosuge K, Murakami T, Kikukawa N, Takemori M. Direct synthesis of porous pure and thiol-functional silica spheres through the $S^+X^-I^+$ assembly pathway. Chem Mater. 2003;15:3184–9.
56. Kosuge K, Kikukawa N, Takemori M. One-step preparation of porous silica spheres from sodium silicate using triblock copolymer templating. Chem Mater. 2004;16:4181–6.
57. Kosuge K, Sato T, Kikukawa N, Takemori M. Morphological control of rod- and fiberlike SBA-15 type mesoporous silica using water-soluble sodium silicate. Chem Mater. 2004;16:899–905.
58. Kresge CT, Leonowicz ME, Roth WJ, Vartuli JC, Beck JS. Ordered mesoporous molecular sieves synthesized by a liquid-crystal template mechanism. Nature. 1992;359:710–2.
59. Kwun I-S, Cho Y-E, Lomeda R-AR, Shin H-I, Choi J-Y, Kang Y-H, Beattie JH. Zinc deficiency suppresses matrix mineralization and retards osteogenesis transiently with catch-up possibly through Runx 2 modulation. Bone. 2010;46(3):732–41.
60. Lebedev OI, Van Tendeloo G, Collart O, Cool P, Vansant EF. Structure and microstructure of nanoscale mesoporous silica sphere. Solid State Sci. 2004;6:489–98.
61. LeGeros RZ. Biologically relevant calcium phosphates: preparation and characterization. In: Myers H, editor. Calcium phosphates in oral biology and medicine, monographs in oral sciences. Basel: Karger; 1991.
62. Liu X, Rahaman MN, Fu QA. Oriented bioactive glass (13-93) scaffolds with controllable pore size by unidirectional freezing of camphene-based suspensions: microstructure and mechanical response. Acta Biomater. 2011;7:406–16.
63. Lopez-Noriega A, Arcos D, Izquierdo-Barba I, Sakamoto Y, Terasaki O, Vallet-Régı M. Ordered mesoporous bioactive glasses for bone tissue regeneration. Chem Mater. 2006;18:3137–44.
64. Lu Y, Ganguli R, Celeste A, Drewien CA, Anderson MT, Brinker CJ, Gong W, Guo Y, Soyez H, Dunn B, Huang MH, Zink JI. Continuous formation of supported cubic and hexagonal mesoporous films by sol–gel dip-coating. Nature. 1997;389:364–8.
65. Ma Y, Qi L, Ma J, Wu Y, Liu O, Cheng H. Large-pore mesoporous silica spheres: synthesis and application in HPLC. Colloids Surf A. 2003;229:1–8.
66. Maeno S, Niki Y, Matsumoto H, Morioka H, Yatabe T, Funayama A, Toyama Y, Taguchi T, Tanaka J. The effect of calcium ion concentration on osteoblast viability, proliferation and differentiation in monolayer and 3D culture. Biomaterials. 2005;26(23):4847–55.
67. Marie PJ. Strontium ranelate: a physiological approach for optimizing bone formation and resorption. Bone. 2006;38(2, Suppl. 1):10–4.
68. Marie PJ. The calcium-sensing receptor in bone cells: a potential therapeutic target in osteoporosis. Bone. 2010;46(3):571–6.
69. Marie PJ, Ammann P, Boivin G, Rey C. Mechanisms of action and therapeutic potential of strontium in bone. Calcif Tissue Int. 2001;69(3):121–9.
70. Meunier PJ, Slosman DO, Delmas PD, Sebert JL, Brandi ML, Albanese C, Lorenc R, Pors-Nielsen S, De Vernejoul MC, Roces A, Reginster JY. Strontium ranelate: dose-dependent effects in established postmenopausal vertebral osteoporosis: a 2-year randomized placebo controlled trial. J Clin Endocrinol Metab. 2002;87(5):2060–6.
71. Moon DS, Lee JK. Tunable synthesis of hierarchical mesoporous silica nanoparticles with radial wrinkle structure. Langmuir. 2012;28:12341–7.
72. Mourino V, Boccaccini AR. Bone tissue engineering therapeutics: controlled drug delivery in three-dimensional scaffolds. J Roy Soc. 2010;7(43):209–27.

73. Mourino V, Newby P, Boccaccini AR. Preparation and characterization of gallium releasing 3-D alginate coated 45S5 bioglass based scaffolds for bone tissue engineering. Adv Eng Mater. 2010;12:B283–91.
74. Mura S, Nicolas J, Couvreur P. Stimuli-responsive nanocarriers for drug delivery. Nat Mater. 2013;12:991–1003. www.nature.com/naturematerials
75. Nakamura T, Mizutani M, Nozaki H, Suzuki N, Yano K. Formation mechanism for monodispersed mesoporous silica spheres and its application to the synthesis of Core/Shell particles. J Phys Chem C. 2007;111:1093–100.
76. Newby CP, Boccaccini AR. Bioactive glass and glass ceramic scaffolds for bone tissue engineering. In: Bioactive glasses – materials properties and applications, a volume in Woodhead publishing series in biomaterials. 2011. p. 107–28.
77. Nielsen FH. Is boron nutritionally relevant? Nutr Rev. 2008;66(4):183–91.
78. Ogawa M. Formation of novel oriented transparent films of layered silica-surfactant nanocomposites. J Am Chem SOC. 1994;116:7941–2.
79. Ogawa M. A simple sol-gel route for the preparation of silica-surfactant mesostructured. Mater Chem Commun. 1996: 1149–50.
80. Ogino M, Ohuchi F, Hench LL. Compositional dependence of the formation of calcium phosphate films on bioglass. J Biomed Mater Res. 1980;14:55–64.
81. Pan W, Ye J, Ning G, Lin Y, Wang J. A novel synthesis of micrometer silica hollow sphere. Mater Res Bull. 2009;44:280–3.
82. Pauwels B, Van Tendeloo G, Thoelen C, Van Rhijn W, Jacobs PA. Structure determination of spherical MCM-41 particles. Adv Mater. 2001;13(17):1317–20.
83. Peltola T, Jokinen M, Rahiala H, Levanen E, Rosenholm JB, Kangasniemi I, Yli-Urpo A. Calcium phosphate formation on porous sol-gel-derived SiO_2 and $CaO\text{-}P_2O_5\text{-}SiO_2$ substrates in vitro. J Biomed Mater Res. 1999;44:12–21.
84. Polshettiwar V, Cha D, Zhang X, Basset JM. High-surface-area silica nanospheres (KCC-1) with a fibrous morphology. Angew Chem Int Ed. 2010;49:9652–6.
85. Rahaman MN, Day DE, Bal BS, Fu Q, Jung SB, Bonewald LF, Tomsia AP. Bioactive glass in tissue engineering. Acta Biomater. 2011;7:2355–73.
86. Rawson H. Inorganic glass-forming system. London: Academic Press; 1967.
87. Reffitt DM, Ogston N, Jugdaohsingh R, Cheung HFJ, Evans BAJ, Thompson RPH, Powell JJ, Hampson GN. Orthosilicic acid stimulates collagen type 1 synthesis and osteoblastic differentiation in human osteoblast-like cells in vitro. Bone. 2003;32(2):127–35.
88. Rodríguez JP, Ríos S, González M. Modulation of the proliferation and differentiation of human mesenchymal stem cells by copper. J Cell Biochem. 2002;85(1):92–100.
89. Ruiz-Hernández E, Baeza A, Vallet-Regí M. Smart drug delivery through DNA/magnetic nanoparticle gates. ACS Nano. 2011;5:1259–66.
90. Salinas AJ, Vallet-Regı M. Bioactive ceramics: from bone grafts to tissue engineering. RSC Adv. 2013;3:11116–31.
91. Schepers EJG, Ducheyne P. Bioactive glass particles of narrow size range for the treatment of oral bone defects: a 1–24 month experiment with several materials and particle sizes and size ranges. J Oral Rehabil. 1997;24:171–81.
92. Schumacher K, Ravikovitch PI, Du Chesne A, Neimark AV, Unger KK. Characterization of MCM-48 materials. Langmuir. 2000;16:4648–54.
93. Sing KSW, Everett DH, Haul RHV, Moscou L, Pierotti RA, Rouquerol J, Siemieniewsk T. Reporting physisorption data for gas/solid systems with special reference to the determination of surface area and porosity. Pure Appl Chem. 1985;57(4):603–19.
94. Stöber W, Fink A, Bohn E. Controlled growth of monodisperse silica spheres in the micron size range. J Colloid Interface Sci. 1968;26:62–9.
95. Tan B, Rankin SE. Interfacial alignment mechanism of forming spherical silica with radially oriented nanopores. J Phys Chem B. 2004;108:20122–9.
96. Tendeloo GV, Lebedev OI, Collart O, Cool P, Vansant EF. Structure of nanoscale mesoporous silica spheres? J Phys Condens Matter. 2003;15:S3037–46. Online at: stacks.iop.org/JPhysCM/15/S3037

97. Tolbert SH, Schaffer TE, Feng J, Hansma PK, Stucky GD. A new phase of oriented mesoporous silicate thin films. Chem Mater. 1997;9:1962–7.
98. Tolli H, Kujala S, Levonen K, Jamsa T, Jalovaara P. Bioglass as a carrier for reindeer bone protein extract in the healing of rat femur defect. J Mater Sci Mater Med. 2010;21(5): 1677–84.
99. Uysal T, Ustdal A, Sonmez MF, Ozturk F. Stimulation of bone formation by dietary boron in an orthopedically expanded suture in rabbits. Angle Orthod. 2009;79(5):984–90.
100. Valerio P, Pereira MM, Goes AM, Leite MF. Effects of extracellular calcium concentration on the glutamate release by bioactive glass (BG60S) preincubated osteoblasts. Biomed Mater. 2009;4:045011.
101. Vallet-Regı M, Ragel CV, Salinas AJ. Glasses with medical applications. Eur J Inorg Chem. 2003;6:1029–42.
102. Vartuli JC, Schmitt KD, Kresge CT, Roth WJ, Leonowicz ME, McCullen SB, Hellring SD, Beck JS, Schlenker JL, Olson DH, Sheppard EW. Development of a formation mechanism for M41S materials. Stud Surf Sci Catal. 1994;84:53–60. http://dx.doi.org/10.1016/S0167-2991(08)64096-3
103. Vivero-Escoto JL, Slowing II, Trewyn BG, Lin VSY. Mesoporous silica nanoparticles for intracellular controlled drug delivery. Small. 2010;6(18):1952–67.
104. Vogel W, Holand W, Nauman K, Gumel J. Development of machineable bioactive glass ceramics for medical uses. J Non Cryst Solids. 1986;80:34–41.
105. Wegst UGK, Ashby MF. The mechanical efficiency of natural materials. Philos Mag. 2004;84(21):2167–81. http://dx.doi.org/10.1080/14786430410001680935
106. Wong PT, Choi SK. Mechanisms of drug release in nanotherapeutic delivery systems. Chem Rev. 2015;115:3388–432. doi:10.1021/cr5004634.
107. Wu C, Ramaswamy Y, Zhu Y, Zheng R, Appleyard R, Howard A, Zreiqat H. The effect of mesoporous bioactive glass on the physiochemical, biological and drug-release properties of poly(DL-lactide-co-glycolide) films. Biomaterials. 2009;30(12):2199–208.
108. Wu C, Zhang Y, Zhou Y, Fan W, Xiao Y. A comparative study of mesoporous-glass/silk and non-mesoporous-glass/silk scaffolds: physiochemistry and in vivo osteogenesis. Acta Biomater. 2011;7(5):2229–36.
109. Wu C, Fan W, Gelinsky M, Xiao Y, Simon P, Schulze R, Doert T, Luo Y, Cuniberti G. Bioactive SrO–SiO_2 glass with well-ordered mesopores: characterization, physiochemistry and biological properties. Acta Biomater. 2011;7(4):1797–806.
110. Xia W, Chang J. Well-ordered mesoporous bioactive glasses (MBG): a promising bioactive drug delivery system. J Control Release. 2006;110(3):522–30.
111. Yamaguchi M. Role of zinc in bone formation and bone resorption. J Trace Elem Exp Med. 1998;11(2e3):119–35.
112. Yamasaki Y, Yoshida Y, Okazaki M, Shimazu A, Uchida T, Kubo T, Akagawa Y, Hamada Y, Takahashi J, Matsuura N. Synthesis of functionally graded $MgCO_3$ apatite accelerating osteoblast adhesion. J Biomed Mater Res. 2002;62(1):99–105.
113. Yan X, Yu C, Zhou X, Tang J, Zhao D. Highly ordered mesoporous bioactive glasses with superior in vitro bone-forming bioactivities. Angew Chem Int Ed. 2004;43:5980–4.
114. Yu C, Fan J, Tian B, Zhao D. Morphology development of mesoporous materials: a colloidal phase separation mechanism. Chem Mater. 2004;16:889–98.
115. Yun H, Kim S, Hyeon Y. Highly ordered mesoporous bioactive glasses with Im3m symmetry. Mater Lett. 2007;61:4569–72.
116. Zhang H, Li Z, Xu P, Wu R, Jiao Z. A facile two step synthesis of novel chrysanthemum-like mesoporous silica nanoparticles for controlled pyrene release. Chem Commun. 2010;46: 6783–5.
117. Zhao D, Feng J, Huo Q, Melosh N, Fredrickson GH, Chmelka BF, Stucky GD. Triblock copolymer syntheses of mesoporous silica with periodic 50 to 300 angstrom pores. Science. 1998;279:548–52.

118. Zhao D, Huo Q, Feng J, Chmelka BF, Stucky GD. Nonionic triblock and star Diblock copolymer and oligomeric surfactant syntheses of highly ordered, hydrothermally stable mesoporous silica structures. J Am Chem Soc. 1998;120:6024–36.
119. Zhao D, Yang P, Chmelka BF, Stucky GD. Multiphase assembly of mesoporous-macroporous membranes. Chem Mater. 1999;11:1174–8.
120. Zhao D, Sun J, Li Q, Stucky GD. Morphological control of highly ordered mesoporous silica SBA-15. Chem Mater. 2000;12:275–9.
121. Zreiqat H, Howlett CR, Zannettino A, Evans P, Schulze-Tanzil G, Knabe C, Shakibaei M. Mechanisms of magnesium-stimulated adhesion of osteoblastic cells to commonly used orthopaedic implants. J Biomed Mater Res. 2002;62(2):175–84.